3f. Acoustic Properties of Solids

W. P. MASON

Columbia University

3f-1. Elastic Constants, Densities, Velocities, and Impedances. Solids are used for conducting acoustic waves in such devices as delay lines useful for storing information and as resonating devices for controlling and selecting frequencies. Acoustic-wave propagation in solids has been used to determine the elastic constants of single crystals and polycrystalline materials. Changes in velocity with frequency and changes in attenuation with frequency have been used to analyze various intergrain, interdomain, and imperfection motions as discussed in Sec. 3f-2.

In an infinite isotropic solid and also in a finite solid for which the wavefront is a large number of wavelengths, plane and nearly plane longitudinal and shear waves can exist which have the velocities

$$v_{\text{long}} = \sqrt{\frac{\lambda + 2\mu}{\rho}} \qquad v_{\text{shear}} = \sqrt{\frac{\mu}{\rho}} \tag{3f-1}$$

where μ and λ are the two Lamé elastic moduli, μ is the shearing modulus, and $\lambda + 2\mu$ has been called the plate modulus. For a rod whose diameter is a small fraction of a wavelength, extensional and torsional waves can be propagated with velocities

$$v_{\text{ext}} = \sqrt{\frac{Y_0}{\rho}} \qquad v_{\text{tor}} = \sqrt{\frac{\mu}{\rho}}$$

where

$$Y_0 = \mu\left(\frac{3\lambda + 2\mu}{\lambda + \mu}\right) \tag{3f-2}$$

For anisotropic media, three waves will, in general, be propagated, but it is only in special cases that the particle motions will be normal and perpendicular to the direction

of propagation. The three velocities satisfy an equation[1]

$$\begin{vmatrix} \lambda_{11} - \rho v^2 & \lambda_{12} & \lambda_{13} \\ \lambda_{12} & \lambda_{22} - \rho v^2 & \lambda_{23} \\ \lambda_{13} & \lambda_{23} & \lambda_{33} - \rho v^2 \end{vmatrix} = 0 \tag{3f-3}$$

where ρ is the density, v the velocity, and the λ's are related to the elastic constants of the crystal by the formulas

$$\begin{aligned}
\lambda_{11} &= l^2c_{11} + m^2c_{66} + n^2c_{55} + 2mnc_{56} + 2nlc_{15} + 2lmc_{16} \\
\lambda_{12} &= l^2c_{16} + m^2c_{26} + n^2c_{45} + mn(c_{46} + c_{25}) + nl(c_{14} + c_{55}) + lm(c_{12} + c_{66}) \\
\lambda_{13} &= l^2c_{15} + m^2c_{46} + n^2c_{35} + mn(c_{45} + c_{36}) + nl(c_{13} + c_{55}) + lm(c_{14} + c_{56}) \\
\lambda_{23} &= l^2c_{56} + m^2c_{24} + n^2c_{34} + mn(c_{44} + c_{23}) + nl(c_{36} + c_{45}) + lm(c_{25} + c_{46}) \\
\lambda_{22} &= l^2c_{66} + m^2c_{22} + n^2c_{44} + 2mnc_{24} + 2nlc_{46} + 2lmc_{26} \\
\lambda_{33} &= l^2c_{55} + m^2c_{44} + n^2c_{33} + 2mnc_{34} + 2nlc_{35} + 2lmc_{45}
\end{aligned} \tag{3f-4}$$

In these formulas c_{11} to c_{66} are the 21 elastic constants and l, m, n the direction cosines of the direction of propagation with respect to the crystallographic x, y, and z axes which are related to the a, b, c crystallographic axes as discussed in an IRE publication.[2]

In Eq. (3f-3), we solve for the quantity ρv^2. It was shown by Christoffel[1] that the direction cosines for the particle motion ξ, i.e., α, β, γ, are related to the λ constants and a solution of ρv^2 by the equations

$$\alpha\lambda_{11} + \beta\lambda_{12} + \gamma\lambda_{13} = \alpha\rho v_i^2;\ \alpha\lambda_{12} + \beta\lambda_{22} + \gamma\lambda_{23} = \beta\rho v_i^2;\ \alpha\lambda_{13} + \beta\lambda_{23} + \gamma\lambda_{33} = \gamma\rho v_i^2 \tag{3f-5}$$

where $i = 1, 2, 3$. Hence, solutions of Eq. (3f-3) are related to particle motions by the equations of (3f-5).

Most metals crystallize in the cubic and hexagonal systems. Furthermore, when a metal is produced by rolling, an alignment of grains occurs such that the rolling direction is a unique axis. This type of symmetry, known as transverse isotropy, results in the same set of constants as that for hexagonal symmetry. For cubic crystals, the resulting elastic constants are

$$c_{11} = c_{22} = c_{33} \qquad c_{12} = c_{13} = c_{23} \qquad c_{44} = c_{55} = c_{66} \tag{3f-6}$$

while for hexagonal symmetry or transverse isotropy, the resulting elastic constants are

$$c_{11} = c_{22}, \qquad c_{12}, \qquad c_{13} = c_{23}, c_{33}, \qquad c_{44} = c_{55}, \qquad c_{66} = \frac{c_{11} - c_{12}}{2} \tag{3f-7}$$

For cubic symmetry, the waves transmitted along the [100] direction and the [110] direction have purely longitudinal and shear components with the elastic-constant values and particle direction ξ given by

[100] direction

$$v_{\text{long}} = \sqrt{\frac{c_{11}}{\rho}} \quad \xi \text{ along } [100] \qquad v_{\text{shear}} = \sqrt{\frac{c_{44}}{\rho}}$$

ξ along any direction in the [100] plane

[1] Love, "Theory of Elasticity," 4th ed., p. 298, Cambridge University Press, New York, 1934.

[2] Standards on Piezoelectric Crystals, *Proc. IRE* **37** (12), 1378–1395 (December, 1949).

[110] direction

$$v_{\text{long}} = \sqrt{\frac{c_{11} + c_{12} + 2c_{44}}{2\rho}} \qquad \xi \text{ along } [110]$$

$$v_{1\,\text{shear}} = \sqrt{\frac{c_{44}}{\rho}} \qquad \xi \text{ along } [001] \qquad v_{2\,\text{shear}} = \sqrt{\frac{c_{11} - c_{12}}{2\rho}}$$

$$\xi \text{ along } [1\bar{1}0]$$

[111] direction

$$v_1 = v_{\text{long}} = \sqrt{\frac{c_{11} + 2c_{12} + 4c_{44}}{3\rho}} \qquad \xi \text{ along } [111]$$

$$v_2 = v_3 = v_{\text{shear}} = \sqrt{\frac{c_{11} - c_{12} + c_{44}}{3\rho}}$$

ξ can be in any direction in the (111) plane.

For hexagonal or transverse isotropy, waves transmitted along the unique axis and any axis perpendicular to this will have the values

[001] direction

$$v_{\text{long}} = \sqrt{\frac{c_{33}}{\rho}} \qquad \xi \text{ along } [001] \qquad v_{\text{shear}} = \sqrt{\frac{c_{44}}{\rho}}$$

ξ along any direction in the [001] plane

[100] direction

$$v_{\text{long}} = \sqrt{\frac{c_{11}}{\rho}} \qquad \xi \text{ along } [100] \qquad v_{1\,\text{shear}} = \sqrt{\frac{c_{44}}{\rho}}$$

$$\xi \text{ along } [001] \qquad v_{2\,\text{shear}} = \sqrt{\frac{c_{11} - c_{12}}{2\rho}} \qquad \xi \text{ along } [010]$$

The fifth constant is measured by transmitting a wave 45 deg between the [100] and [001] directions; i.e., $l = n = 1/\sqrt{2}$; $m = 0$. For this case

$$\lambda_{11} = \frac{c_{11} + c_{44}}{2} \qquad \lambda_{12} = \lambda_{23} = 0 \qquad \lambda_{13} = \frac{c_{13} + c_{44}}{2} \qquad \lambda_{22} = \frac{c_{11} - c_{12} + 2c_{44}}{4}$$

$$\lambda_{33} = \frac{c_{44} + c_{33}}{2} \tag{3f-8}$$

The three solutions of Eq. (3f-3) are

$$\rho v_1^2 = \frac{c_{11} - c_{12} + 2c_{44}}{4}$$

$$\rho v_{2,3}^2 = \frac{[(c_{11} + c_{33} + 2c_{44})/2] \pm \sqrt{[(c_{11} - c_{33})/2]^2 + (c_{13} + c_{44})^2}}{2} \tag{3f-9}$$

For these three velocities, the particle velocities have the direction cosines

For v_1, $\quad \beta = 1$

For v_2, $\quad \alpha = \gamma \left\{ \frac{c_{11} - c_{33}}{2(c_{13} + c_{44})} + \sqrt{1 + \left[\frac{c_{11} - c_{33}}{2(c_{13} + c_{44})}\right]} \right\}$ (3f-10)

For v_3, $\quad \alpha = -\gamma \left\{ \frac{c_{33} - c_{11}}{2(c_{13} + c_{44})} + \sqrt{1 + \left[\frac{(c_{11} - c_{33})^2}{2(c_{13} + c_{44})}\right]} \right\}$

Hence, unless c_{11} is nearly equal to c_{33}, a longitudinal or shear crystal will generate both types of waves. Experimentally, however, it is found that a good discrimination can be obtained against the type of wave that is not primarily generated and a single velocity can be measured. A resonance technique can also be used to evaluate all the elastic constants of a crystalline material.

TABLE 3f-1. DENSITIES OF GLASSES, PLASTICS, AND METALS IN POLYCRYSTALLINE AND CRYSTALLINE FORM (X-RAY DENSITIES FOR CRYSTALS)*

Materials	Composition	Temp., °C	Density, 10^3 kg/m^3 or g/cm^3
Aluminum			
Hard-drawn	.....	20	2.695
Crystal	.....	25	2.697
Aluminum and copper	10 Al, 90 Cu	..	7.69
	5 Al, 95 Cu	..	8.37
	3 Al, 97 Cu	..	8.69
Beryllium	.....	20	1.87
Crystal	.....	18	1.871
Brass:			
Yellow	70 Cu, 30 Zn	..	8.5–8.7
Red	90 Cu, 10 Zn	..	8.6
White	50 Cu, 50 Zn	..	8.2
Bronze	90 Cu, 10 Sn	..	8.78
	85 Cu, 15 Sn	..	8.89
	80 Cu, 20 Sn	..	8.74
	75 Cu, 25 Sn	..	8.83
Chromium	.....	20	6.92–7.1
Crystal	.....	18	7.193
Cobalt	.....	21	8.71
Crystal	.....	..	8.788
Constantan	60 Cu, 40 Ni	..	8.88
Copper	.....	..	8.3–8.93
Crystal	.....	18	8.936
Duralumin	17ST = 4 Cu, 0.5 Mg, 0.5 Mn	..	2.79
Germanium	.....	..	5.3
Crystal	.....	20	5.322
German silver	26.3 Cu, 36.6 Zn, 36.8 Ni	..	8.30
	52 Cu, 26 Zn, 22 Ni	..	8.45
	59 Cu, 30 Zn, 11 Ni	..	8.34
	63 Cu, 30 Zn, 6 Ni	..	8.30
Gold	.....	..	18.9–19.3
Crystal	.....	20	19.32
Indium	.....	..	7.28
Crystal	.....	..	7.31
Invar	63.8 Fe, 36 Ni, 0.20 C	..	8.0
Iron	.....	20	7.6–7.85
Crystal	.....	20	7.87
Lead	.....	20	11.36
Crystal	.....	18	11.34
Lead and tin	87.5 Pb, 12.5 Sn	..	10.6
	84 Pb, 16 Sn	..	10.33
	72.8 Pb, 22.2 Sn	..	10.05
	63.7 Pb, 36.3 Sn	..	9.43
	46.7 Pb, 53.3 Sn	..	8.73
	30.5 Pb, 69.5 Sn	..	8.24

TABLE 3f-1. DENSITIES OF GLASSES, PLASTICS, AND METALS IN POLYCRYSTALLINE AND CRYSTALLINE FORM (X-RAY DENSITIES FOR CRYSTALS)* (*Continued*)

Materials	Composition	Temp., °C	Density, 10^3 kg/m^3 or g/cm^3
Magnesium	.....	..	1.74
Crystal	.....	25	1.748
Manganese	.....	..	7.42
Crystal	.....	..	7.517
Mercury	.....	20	13.546
Monel metal	71 Ni, 27 Cu, 2 Fe	..	8.90
Molybdenum	.....	..	10.1
Crystal	.....	25	10.19
Nickel	.....	..	8.6–8.9
Crystal	.....	25	8.905
Nickel silver	.....	..	8.4
Phosphor bronze	79.7 Cu, 10 Sn, 9.5 Sb, 0.8 P	..	8.8
Platinum	.....	20	21.37
Crystal	.....	18	21.62
Silicon	.....	15	2.33
Crystal	.....	25	2.332
Silver	.....	..	10.4
Crystal	.....	25	10.49
Steel K9	.....	..	7.84
347 stainless steel	.....	..	7.91
Tin	.....	..	7–7.3
Crystal	.....	..	7.3
Titanium	.....	..	4.50
Tungsten	.....	..	18.6–19.1
Crystal	.....	25	19.2
Tungsten carbide	.....	..	13.8
Zinc	.....	..	7.04–7.18
Crystal	.....	25	7.18
Fused silica	.....	..	2.2
Pyrex glass (702)	.....	..	2.32
Heavy silicate flint	.....	..	3.879
Light borate crown	.....	..	2.243
Lucite	.....	..	1.182
Nylon 6-6	.....	..	1.11
Polyethylene	.....	.	0.90
Polystyrene	.....	..	1.056

* See also Tables 2b-1 through 2b-13.

When a longitudinal or shear wave is reflected at an angle from a plane surface, both a longitudinal and a shear wave will in general be reflected from the surface, the angles of reflection and refraction satisfying Snell's law

$$\frac{\sin \beta}{v_S} = \frac{\sin \alpha}{v_l} \tag{3f-11}$$

where α and β are the angles of incidence and refraction with respect to a normal to the reflecting surface. Exceptions to this rule occur if a shear wave has its direction of particle displacement parallel to the reflecting surface, in which case only a pure shear wave is reflected, with the angle of reflection being equal to the angle of incidence. Use is made of this result in constructing delay lines which can be contained in a small volume. When the direction of transmission is normal to the surface, the incident wave is reflected without change of mode. If the transmitting medium is connected to another medium with different properties, the transmission and reflection factors are determined by the relative impedances of the two media. The impedance is given by the formula

$$Z = \rho v = \sqrt{E\rho} \tag{3f-12}$$

where E is the appropriate elastic stiffness and ρ the density. The reflection and transmission coefficients between medium 1 and medium 2 are given by the equations

$$R = \frac{Z_1 - Z_2}{Z_1 + Z_2} \qquad T = 1 - R = \frac{2Z_2}{Z_1 + Z_2} \tag{3f-13}$$

Tables 3f-1 to 3f-4 list the densities, elastic constants, velocities, and impedances for a number of materials used in acoustic-wave propagation.

3f-2. Attenuation Due to Thermal Effects, Relaxations, and Scattering. When sound is propagated through a solid, it suffers a conversion of mechanical energy into heat. While all the causes of conversion are not known, a number of them are, and tables for these effects are given in this section.

3f-3. Loss Due to Heat Flow. When a sound wave is sent through a body, a compression or rarefaction occurs which heats or cools the body. This heat causes thermal expansions which alter slightly the elastic constants of the material. Since the compressions and rarefactions occur very rapidly, there is not time for much heat to flow and the elastic constants measured by sound propagation are the adiabatic constants. For an isotropic material, the adiabatic constants are related to the isothermal constants by the formulas[1]

$$\lambda^\sigma = \lambda^\theta + \frac{9\alpha^2 B^2 \Theta}{\rho C_v} \qquad \mu^\sigma = \mu^\theta \qquad Y_0^\sigma = Y_0^\theta + \left(\frac{\mu}{\lambda + \mu}\right)^2 \frac{9\alpha^2 B^2 \Theta}{\rho C_v} \tag{3f-14}$$

where the superscripts σ and θ indicate adiabatic and isothermal constants, α is the linear temperature coefficient of expansion, B the bulk modulus ($B = \lambda + \frac{2}{3}\mu$), Θ the absolute temperature in kelvins, ρ the density, and C_v the specific heat at constant volume. Table 3f-5 shows these quantities for a number of materials.

The difference between λ^σ and λ^θ should be taken account of when one compares the elastic constants measured by ultrasonic means with those measured by static means. From the data given in Table 3f-5, it is evident that this effect can produce errors as high as 10 percent in the case of zinc. Adiabatic elastic constants are measured from frequencies somewhat less than those for which thermal equilibrium is established during the cycle up to a frequency[1] $f \doteq (\sigma C_v v^2/2\pi K)$ for which wave propagation takes place isothermally. This latter frequency is approximately 10^{12} Hz for most metals.

When account is taken of the energy lost by heat flow between the hot and cool parts, this adds an attenuation for longitudinal waves equal to

$$A = \frac{2\pi f^2}{\rho v^3}\left[\frac{K}{C_v}\left(\frac{E^\sigma - E^\theta}{E^\theta}\right)\right] \quad \text{nepers/m} \tag{3f-15}$$

[1] W. P. Mason, "Piezoelectric Crystals and Their Application to Ultrasonics," pp. 480–481. D. Van Nostrand Company, Inc., Princeton, N.J., 1950.

TABLE 3f-2. ELASTIC CONSTANTS, WAVE VELOCITIES, AND CHARACTERISTIC IMPEDANCES OF METALS, GLASSES, AND PLASTICS

Materials	$Y_0 \times 10^{-10}$ newton/m²	$\mu \times 10^{-10}$ newton/m²	$\lambda \times 10^{-10}$ newton/m²	Poisson's ratio, σ	$V_l = \sqrt{(\lambda + 2\mu)/\rho}$, m/sec	$V_s = \sqrt{\mu/\rho}$, m/sec	$V_{ext} = \sqrt{Y_0/\rho}$, m/sec	$Z_l = \sqrt{\rho(\lambda + 2\mu)}$, 10^6 kg/sec m²	$Z_s = \sqrt{\rho\mu}$, 10^6 kg/sec m²
Aluminum, rolled	6.8–7.1	2.4–2.6	6.1	0.355	6,420	3,040	5,000	17.3	8.2
Beryllium	30.8	14.7	1.6	0.05	12,890	8,880	12,870	24.1	16.6
Brass, yellow, 70 Cu, 30 Zn	10.4	3.8	11.3	0.374	4,700	2,110	3,480	40.6	18.3
Constantan	16.1	6.09	11.4	0.327	5,177	2,625	4,270	45.7	23.2
Copper, rolled	12.1–12.8	4.6	13.1	0.37	5,010	2,270	3,750	44.6	20.2
Duralumin 17S	7.15	2.67	5.44	0.335	6,320	3,130	5,150	17.1	8.5
Gold, hard-drawn	8.12	2.85	15.0	0.42	3,240	1,200	2,030	62.5	23.2
Iron, cast	15.2	5.99	6.92	0.27	4,994	2,809	4,480	37.8	21.35
Iron electrolytic	20.6	8.2	11.3	0.29	5,950	3,240	5,120	46.4	25.3
Armco	21.2	8.24	11.35	0.29	5,960	3,240	5,200	46.5	25.3
Lead, rolled	1.5–1.7	0.54	3.3	0.43	1,960	690	1,210	22.4	7.85
Magnesium, drawn, annealed	4.24	1.62	2.56	0.306	5,770	3,050	4,940	10.0	5.3
Monel metal	16.5–18	6.18–6.86	12.4	0.327	5,350	2,720	4,400	47.5	24.2
Nickel	21.4	8.0	16.4	0.336	6,040	3,000	4,900	53.5	26.6
Nickel silver	10.7	3.92	11.2	0.37	4,760	2,160	3,575	40.0	18.1
Platinum	16.7	6.4	9.9	0.303	3,260	1,730	2,800	69.7	37.0
Silver	7.5	2.7	8.55	0.38	3,650	1,610	2,680	38.0	16.7
Steel, K9	21.6	8.29	10.02	0.276	5,941	3,251	5,250	46.5	25.4
347 stainless steel	19.6	7.57	11.3	0.30	5,790	3,100	5,000	45.7	24.5
Tin, rolled	5.5	2.08	4.04	0.34	3,320	1,670	2,730	24.6	11.8
Titanium	11.6	4.40	7.79	0.32	6,070	3,125	5,090	27.3	14.1
Tungsten, drawn	36.2	13.4	31.3	0.35	5,410	2,640	4,320	103	50.5
Tungsten carbide	53.4	21.95	17.1	0.22	6,655	3,984	6,240	91.8	55.0
Zinc, rolled	10.5	4.2	4.2	0.25	4,210	2,440	3,850	30	17.3
Fused silica	7.29	3.12	1.61	0.17	5,968	3,764	5,760	13.1	8.29
Pyrex glass	6.2	2.5	2.3	0.24	5,640	3,280	5,170	13.1	7.6
Heavy silicate flint	5.35	2.18	1.77	0.224	3,980	2,380	3,720	15.4	9.22
Light borate crown	4.61	1.81	2.2	0.274	5,100	2,840	4,540	11.4	6.35
Lucite	0.40	0.143	0.562	0.4	2,680	1,100	1,840	3.16	1.3
Nylon 6–6	0.355	0.122	0.511	0.4	2,620	1,070	1,800	2.86	1.18
Polyethylene	0.076	0.026	0.288	0.458	1,950	540	920	1.75	0.48
Polystyrene	0.360	0.133	0.319	0.353	2,350	1,120	1,840	2.49	1.19

TABLE 3f-3. ELASTIC CONSTANTS OF CUBIC SINGLE CRYSTALS*

(s = compliance modulus, m²/newton; c = stiffness modulus, newtons/m²; for cgs units of dynes/cm², multiply the c tabular entries by 10; divide the s tabular entries by 10 to obtain cm²/dyne)

Crystal		$s_{11} \times 10^{11}$	$s_{12} \times 10^{11}$	$s_{44} \times 10^{11}$	$c_{11} \times 10^{-10}$	$c_{12} \times 10^{-10}$	$c_{44} \times 10^{-10}$	$B = [(c_{11} + 2c_{12})/3] \times 10^{-10}$	Anisotropy $2c_{44}/(c_{11} - c_{12})$
Ag		2.32	−0.993	2.29	11.9	8.94	4.37	9.93	2.95
Al		1.59	−0.58	3.52	10.82	6.13	2.85	7.69	1.24
Au		2.33	−1.07	2.38	19.6	16.45	4.20	17.5	2.67
Cu		1.49	−0.625	1.33	17.02	12.3	7.51	13.9	3.18
Fe		0.757	−0.282	0.862	23.7	14.1	11.6	17.3	2.37
Ge		0.964	−0.260	1.49	12.92	4.79	6.70	7.50	1.65
K		83.3	−37.0	38.0	0.416	0.333	0.263	0.361	6.34
Na		48.3	−20.9	16.85	0.615	0.469	0.592	0.518	8.11
Ni (sat.)		0.80	−0.312	0.844	25.0	16.0	11.85	19.0	2.63
Pb		9.30	−4.26	6.94	4.85	4.09	1.44	4.34	3.79
Si		0.768	−0.214	1.26	16.57	6.39	7.956	9.783	1.56
W		0.257	−0.073	0.66	50.2	19.9	15.15	30.0	1.0
Diamond†		0.0958	−0.01	0.174	107.6	12.5	57.6	44.2	1.21
NaCl		2.4	−0.50	7.8	4.9	1.24	1.26	2.5	0.688
KBr		4.0	−1.2	7.5	3.5	0.58	0.50	1.6	0.342
KCl		2.7	−0.3	15.6	4.0	0.62	0.62	1.7	0.361
Alloy	Atom % of second component	Elastic Constants of Copper Alloys‡							
CuZn	4.53	1.59	−0.671	1.348	16.34	11.92	7.42	13.39	3.36
CuAl	4.81	1.59	−0.674	1.335	16.58	12.16	7.49	13.63	3.39
	9.93	1.67	−0.711	1.305	15.95	11.77	7.66	13.16	3.66
CuGa	1.58	1.55	−0.65	1.346	16.49	11.93	7.43	13.45	3.25
	4.15	1.59	−0.672	1.349	16.51	12.10	7.41	13.57	3.36
CuSi	4.17	1.61	−0.685	1.336	16.78	12.42	7.48	13.87	3.43
	5.16	1.67	−0.709	1.335	16.09	11.88	7.49	13.28	3.56
	7.69	1.73	−0.745	1.350	16.64	12.60	7.41	13.95	3.67
CuGe	1.03	1.52	−0.637	1.333	16.66	12.00	7.50	13.62	3.29
	1.71	1.57	−0.663	1.333	16.30	11.83	7.50	13.32	3.35

* See also Tables 2e-1 through 2e-6.
† Recent data by W. L. Bond and H. J. McSkimin.
‡ Data from C. S. Smith.

TABLE 3f-4. ELASTIC CONSTANTS OF HEXAGONAL CRYSTALS

(s = compliance moduli, m²/newton; c = stiffness moduli, newtons/m²; for cgs units of dynes/cm² multiply the c tabular entries by 10; divide the s tabular entries by 10 to obtain cm²/dyne)

Crystal	$s_{11} \times 10^{11}$	$s_{12} \times 10^{11}$	$s_{13} \times 10^{11}$	$s_{33} \times 10^{11}$	$s_{44} \times 10^{11}$	
Cd	1.23	−0.15	−0.93	3.55	5.40	
Mg	2.21	−0.77	−0.49	1.97	6.03	
Zn	0.84	+0.11	−0.78	2.87	2.64	
Co	0.473	−0.231	−0.07	0.319	1.325	
	$c_{11} \times 10^{-10}$	$c_{12} \times 10^{-10}$	$c_{13} \times 10^{-10}$	$c_{33} \times 10^{-10}$	$c_{44} \times 10^{-10}$	$B = \dfrac{1}{2(s_{11} + s_{12}) + s_{33} + 4s_{13}} \times 10^{-10}$
Cd	12.12	4.81	4.42	4.45	1.85	5.03
Mg	5.86	2.49	2.08	6.60	1.65	3.46
Zn	16.35	2.64	5.17	5.31	3.78	8.26
Co	30.71	16.5	10.27	35.81	7.55	19.01

TABLE 3f-5. ADIABATIC AND ISOTHERMAL ELASTIC CONSTANTS AND ATTENUATION DUE TO HEAT FLOW

Material	$10^{-3} \times$ density, kg/m^3	C_v, joules/kg/°C $\times 10^{-3}$	$\alpha \times 10^6$ 1/°C	$K \times 10^{-2}$ watts/m^2/m/°C	$\lambda^\theta \times 10^{-10}$ newtons/m^2	$\mu \times 10^{-10}$ newtons/m^2	$(\lambda^\sigma - \lambda^\theta) \times 10^{-9}$ newtons/m^2	$(Y_0^\sigma - Y_0^\theta) \times 10^{-8}$ newtons/m^2	A/f^2, nepers/m
Aluminum	2.699	0.9	23.9	2.22	6.1	2.5	3.8	3.2	2.3×10^{-16}
Beryllium	1.82	2.17	12.4	1.58	1.6	14.7	1.4	11.4	2.1×10^{-18}
Copper	8.96	0.384	16.5	3.93	13.1	4.6	5.5	3.7	4.45×10^{-16}
Gold	19.32	0.13	14.2	2.97	15.0	2.85	6.1	1.5	1.95×10^{-15}
Iron	7.87	0.46	11.7	0.75	11.3	8.2	2.7	4.3	1.88×10^{-17}
Lead	11.4	0.128	29.4	0.344	3.3	0.54	2.12	0.36	2.95×10^{-15}
Magnesium	1.74	1.04	26	1.59	2.56	1.62	1.3	2.1	2.0×10^{-16}
Nickel	8.90	0.44	13.3	0.92	16.4	8.0	5.7	6.1	3.8×10^{-17}
Silver	10.49	0.234	19.7	4.18	8.55	2.7	4.5	2.6	1.95×10^{-15}
Tin	7.3	0.225	23	0.67	4.04	2.08	3.5	4.0	9.7×10^{-16}
Tungsten	19.3	0.134	4.3	2.0	31.3	13.4	3.1	2.8	5.0×10^{-17}
Zinc	7.1	0.382	29.7	1.12	4.2	4.2	4.3	10.7	3.8×10^{-16}
Fused silica	2.2	0.92	0.5	0.01	1.61	3.12	0.00045	0.002	2.6×10^{-22}

TABLE 3f-6. FACTORS GOVERNING INTERGRAIN HEAT FLOW IN METALS

Metal	Pb	Ag	Cu	Au	Fe	Al	W
R	0.065	0.031	0.031	0.014	0.022	0.0009	10^{-1}
$(C_p - C_v)/C_v$	0.067	0.040	0.028	0.038	0.016	0.046	0.006
Product	4.4×10^{-3}	1.2×10^{-3}	8.7×10^{-4}	5.3×10^{-4}	3.5×10^{-4}	4×10^{-5}	6×10^{-9}

where f is the frequency, v the velocity, K the heat conductivity, and E the appropriate elastic constant for the mode of propagation considered. Since $Q = B/2A$, it becomes

$$Q = \frac{\rho C_v v^2}{2fK[(E^\sigma - E^\theta)/E^\theta]} \tag{3f-16}$$

where Q is the ratio of 2π times the energy stored to energy dissipated per cycle and B is the phase shift per unit length. Table 3f 5 shows the attenuation for a number of solids due to thermoelastic loss.

The thermoelastic effect produces about half the thermal attenuation for metals but only about 4 percent for dielectric crystals. The largest source of loss for these crystals is the Akhieser effect which results from an instantaneous separation of the phonon modes, followed by an equilibration of these temperatures which occurs with a relaxation time τ. This effect produces a loss of about 40 times the thermoelastic loss for insulators. According to a recent theory[1] this loss is

$$\alpha_{(\text{nep./cm})} = \frac{\omega^2 D(E_0 K/C_v \bar{v}^2)}{2\rho v^3(1 + \omega^2\tau^2)} \qquad \tau = \frac{3K}{C_v \bar{v}^2} \tag{3f-17}$$

where the ratio of the total thermal energy E_0 to the specific heat C_v is proportional to a factor F times the absolute temperature T. F varies from 0.25 at very low temperatures to unity above the Debye temperature. D is a nonlinear constant which can be calculated when the third-order moduli of the material are known, K is the thermal conductivity, ρ the crystal density, v is the sound velocity, and $\bar{v}$ the Debye average velocity. A number of third-order moduli have been measured for at least six crystals, and the agreement with Eq. (3f-17) is good.

Figure 3f-1 shows typical measurements of the attenuation of the two shear waves and the longitudinal wave in a single crystal of aluminum oxide Al_2O_3. Below 20 to 30 K the attenuation is independent of the temperature. This region is assumed to be controlled by scattering losses due to imperfections in the crystal and transducers. This loss is a good measure of the imperfections in the crystal. Above this region the attenuation for the slow shear wave increases as the fourth power of the temperature from 20 to 80 K. This is in agreement with the theory of Landau and Rumer (1937),[2] which considers the direct interactions of the acoustic waves with the thermal phonons. This formula can be put into the form

$$\alpha = 60\gamma^2 \frac{kT}{Mv^2}\left(\frac{T}{\theta}\right)^3 \frac{2\pi}{\lambda} \tag{3f-18}$$

where α is the attenuation in nepers per cm, γ the Gruencisen constant, k the Boltzmann constant, M the average atomic mass, $\bar{v}$ an average sound velocity, T the absolute temperature, θ the Debye temperature, and λ the acoustic wavelength. The agreement with the formula is quite good. The fast shear wave and the longitudinal wave behave in a different manner with slopes proportional to T^7 and T^9, respectively. Explanations for these values have not yet been obtained.

For higher temperatures when the product of the angular frequency ω times the thermal relaxation time τ is much less than unity, individual interactions between sound waves and phonons can no longer be followed. In this region the two effects causing the thermal attenuation are the thermoelastic effect and the Akhieser effect, discussed above.

3f-4. Loss Due to Intergrain Heat Flow. A related thermal loss that occurs in polycrystalline material is the thermoelastic relaxation loss which arises from heat flow

[1] See W. P. Mason, "Physical Acoustics," vol. IIIB, chap. 6, Academic Press, Inc., New York, 1965.

[2] L. Landau and G. Rumer, *Physik. Z. Sowjetunion* **11**, 18 (1937).

from grains that have received more compression or extension in the course of the wave motion than do adjacent grains. The Q from this source has been shown to be[1]

$$\frac{1}{Q} = \frac{C_p - C_v}{C_v} R \frac{f_0 f}{f_0^2 + f^2} \tag{3f-19}$$

where R is that fraction of the total strain energy which is associated with the fluctuations of dilations, and f_0, the relaxation frequency, is approximately

$$f_0 = \frac{D}{L_c^2} = \frac{K}{\rho C_p L_c^2} \tag{3f-20}$$

where L_c is the mean diameter of the crystallites and D the diffusion constant.

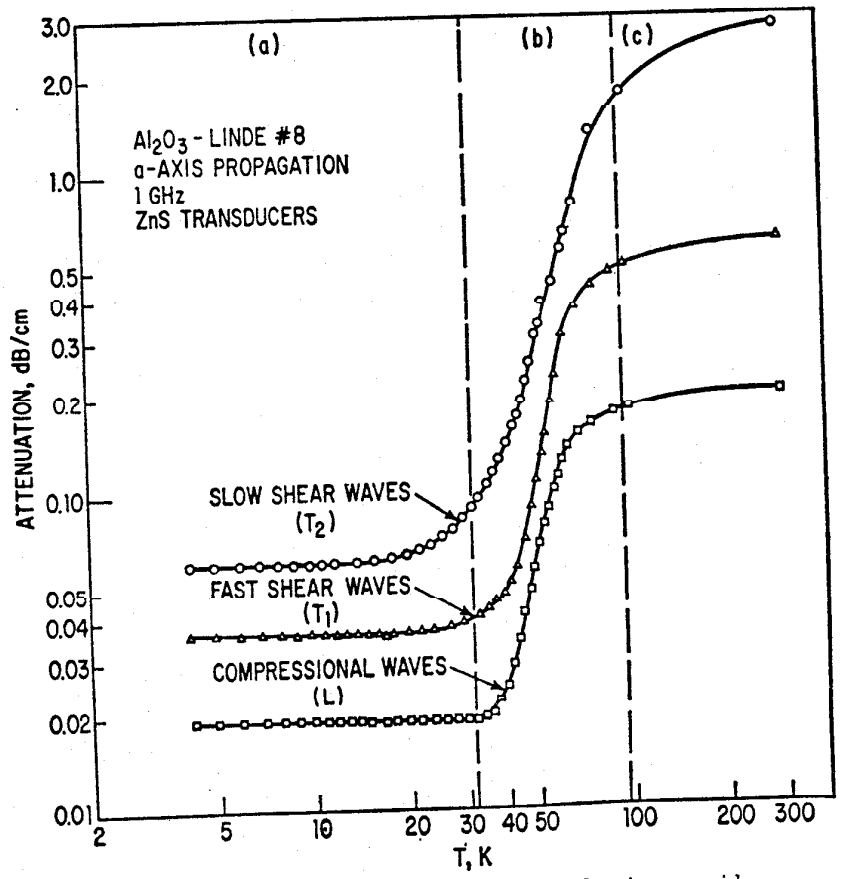

FIG. 3f-1. Attenuation of plane waves in aluminum oxide.

For most materials, the relaxation frequencies are under 100 kHz. Table 3f-6 gives the product $[(C_p - C_v)/C_v]R$ for a number of metals.

3f-5. Loss Due to Grain Rotation. Another source of loss due to grain structure in metals is the loss due to the viscosity of the boundary layer between grains. This allows a relative rotation of grains provided the relaxation time is comparable to the time of the applied force. Figure 3f-1 shows the elastic modulus and the associated Q of a polycrystalline aluminum rod in torsional vibration at a frequency of 0.8 Hz as compared with similar measurements for a single crystal. The relaxation time for grain-boundary rotation is a function of temperature according to the equation

$$\tau = \tau_0 e^{H/kT} \tag{3f-21}$$

[1] C. Zener, "Elasticity and Anelasticity of Metals," p. 84, University of Chicago Press Chicago, 1948.

where H, the activation energy, is of the same order as that found for creep and self-diffusion.

3f-6. Loss Due to Grain Scattering of Sound. Another effect of grain structure in solids is a loss of energy from the main wave due to the scattering of sound when the sound wavelength is of the same order as the grain size. This scattering occurs because adjacent grains have different orientations, and a reflection of sound occurs because of the resulting impedance difference between grains. An approximate formula[1] holding when the wavelength is larger than three times the grain size, and multiple scattering is neglected, is

$$\alpha_s \doteq \frac{8\pi^4 L_c^3 f^4}{9v^4} S \qquad \text{nepers/m} \tag{3f-22}$$

where L_c is the average grain diameter, f the frequency, v the velocity, and S a scattering factor related to the anisotropy of the metal. The scattering factor taking account of mode conversion has been calculated for cubic and hexagonal crystals.[2] Since the formulas are complicated, the reader is referred to a recent review article.[3]

The formula (3f-22) is valid in the Rayleigh scattering region when the wavelength is three times or larger than the grain diameter. For higher frequencies the attenuation increases proportional to the square of the frequency and finally becomes independent of the frequency for high frequencies.

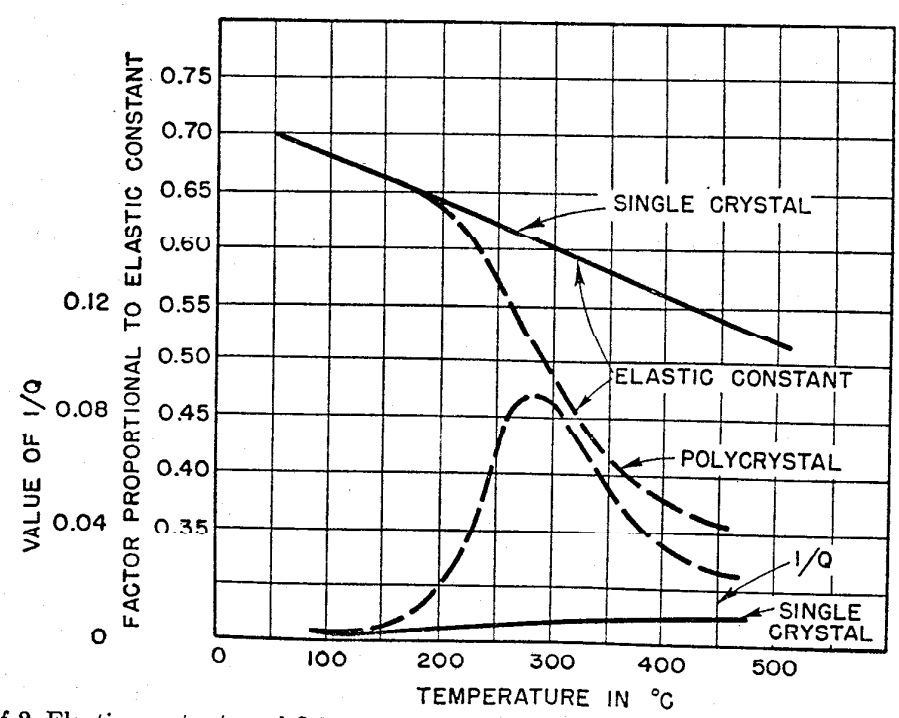

FIG. 3f-2. Elastic constants and Q for single-crystal and polycrystal aluminum. (*After Ké.*)

3f-7. Acoustic Losses in Ferromagnetic and Ferroelectric Materials. Stresses in ferromagnetic and ferroelectric materials can cause motion of domain walls or rota tion of domain directions. These occur in such a manner that domains are strengthened in directions parallel, antiparallel, or perpendicular to the direction of the stress. The

[1] Mason, *op. cit.*, p. 422.

[2] L. G. Merkulov, *Soviet Phys.—Tech. Phys.* (English Translation) **1**, 59–69 (1950).

[3] See Emmanuel P. Papadakis, "Physical Acoustics," vol. IVB, chap. 15, Academic Press, Inc., New York, 1968.

increased polarization in the direction of the stress produces increased strains which are the same sign in both parallel and antiparallel domains since magnetostriction and electrostriction are square-law effects and hence the elastic stiffnesses of demagnetized materials are less than those of completely magnetized materials. For polarizations directed along cube axes, the difference in elastic constants for the saturated and depolarized states, i.e., the ΔE effect, is[1]

$$\frac{\Delta E}{E_D} = \frac{9\mu\lambda_s^2 E_s}{20\pi P_s^2} \tag{3f-23}$$

where μ is the initial permeability or dielectric constant, λ_s the saturated change in length along a polycrystalline rod, E_s and E_D the saturated and demagnetized elastic-stiffness constant, and P_s the saturated magnetic or electric polarization. When the polarization lies along a cube diagonal—as in nickel—λ_s is replaced by $\frac{2}{3}\lambda_{111}[5c_{44}/(c_{11} - c_{12} + 3c_{44})]$ where λ_{111} is the saturated increase in length along the [111] direction and $5c_{44}/(c_{11} - c_{12} + 3c_{44})$ is a ratio of elastic constants.

The motion of walls or the rotation of domains in metallic ferromagnetic materials generates eddy currents and hence causes an acoustic loss. It has been shown that the permeability follows a relaxation equation

$$\mu = \mu_0 \frac{1 - jf/f_0}{1 + f^2/f_0^2} \tag{3f-24}$$

where $f_0 \doteq 4R/25\mu_0 L_c^2$, R is the resistivity, L_c is the domain diameter, and $j^2 = -1$. For a distribution of domain sizes

$$\mu = \mu_0 \sum_{i=1}^{m} \frac{V_i}{V} \frac{1 - jf/f_i}{1 + f^2/f_i^2} \tag{3f-25}$$

where V_i is the volume occupied by domains of size L_i and V is the total volume.

Inserting in Eq. (3f-23) the $\Delta E/E_D$ and Q are given by

$$\frac{\Delta E}{E_D} = \frac{9\lambda_s^2 E_s}{20\pi P_s^2}\left(\sum_{i=1}^{m} \frac{V_i/V}{1 + f^2/f_i^2}\right); \qquad \frac{1}{Q} = \frac{9\lambda_s^2 E_s}{20\pi P_s^2}\left[\sum \frac{(V_i/V)(f/f_i)}{1 + (f/f_i)^2}\right] \tag{3f-26}$$

Figure 3f-3 shows measurements of the ΔE effect and the decrement $\delta = \pi/Q$ plotted over a frequency range, for a polycrystalline nickel rod.

Another effect causing losses in ferromagnetic and ferroelectric materials is the microhysteresis effect. In this effect the domain walls or domain rotations lag behind the applied stress and produce a hysteresis loop. Hence the initial susceptibility has a hysteresis component which is a function of the amount of stress. Average values of the parameters can be written in the form

$$\mu = \mu_0[1 - jf(A)] \tag{3f-27}$$

where $f(A)$ is a function of the amplitude. Inserting this value of μ in Eq. (3f-23), the value of the microhysteresis loss is given. This type of loss is present in ferroelectric materials and is the principal cause of the low mechanical Q.

3f-8. Other Types of Losses. In addition to these recognized types of losses, other types exist which appear to be associated with the motion of dislocations. Figure 3f-4 shows the Q of a number of materials measured[2] in a frequency range from 10^3 to

[1] R. M. Bozorth, "Ferromagnetism," p. 691, D. Van Nostrand Company, Inc., Princeton, N.J., 1951.

[2] R. L. Wegel and H. Walter, *Physics* **6**, 141 (1953).

10^5 Hz for small strains. Except for nickel and iron rods, whose decrease in Q with increase in frequency is accounted for by microeddy-current effects, the materials have a Q nearly independent of frequency. When a single or polycrystal sample is strained, an internal friction peak develops, as shown by Fig. 3f-5, whose peak temperature depends on the frequency. This peak, known as the Bordoni peak after its discoverer,[1] is believed to be due to the motion of dislocation segments from one minimum energy position in the crystal to adjacent ones under the combined action of thermal and mechanical applied stresses. This action takes place over the Peierl barrier which determines the forces returning the dislocations to their minimum energy positions. In fact, the Bordoni peak measurements provide the most reliable estimates of the Peierl barrier values. At high frequencies and for pure materials, the internal friction is determined by the damping of dislocation loops[2] by loss of energy to phonons and electrons.

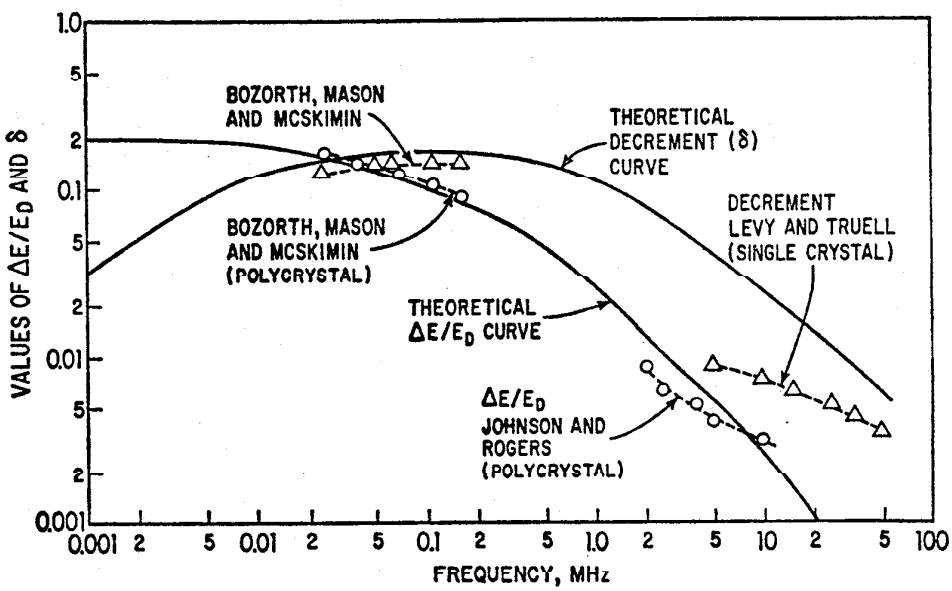

FIG. 3f-3. Decrement and ΔE effect as a function of frequency for polycrystal rod. (*After Bozorth, Mason, and McSkimin; Johnson and Rogers; and Levy and Truell.*)

Other internal friction effects and modulus changes occur for higher strain levels and elevated temperatures as shown by Fig. 3f-6. These are usually ascribed[3] to the pulling of dislocations away from pinning impurity atoms by stresses and thermal agitation. For still higher stresses, Frank-Read sources can be actuated, and these result in a region of very rapidly rising internal friction accompanied by fatigue of the material which occurs for a sufficiently large number of cycles.

Attenuation at Low Temperatures. At very low temperatures, the ultrasonic attenuation of pure normally conducting metals becomes high. Figure 3f-7 shows measurements of pure tin for two directions in the crystal and for two frequencies. Above 10 K, the ultrasonic attenuation is relatively small and increases as the square of the frequency. At 4 K, at which tin is still in the normal state, the attenuation is high and increases in proportion to the frequency. It has been shown that the

[1] P. G. Bordoni, *J. Acoust. Soc. Am.* **26**(4), 495 (July, 1954).

[2] See A. V. Granato and K. Lücke, "Physical Acoustics," vol. IVA, chap. 6, Academic Press, Inc., New York, 1968.

[3] See Warren P. Mason, "Physical Acoustics and the Properties of Solids," chap. 9, D. Van Nostrand Company, Inc., Princeton, N.J., 1958.

added attenuation in the normal state is due to the transfer of momentum and energy from the acoustic wave to the free electrons in the metal. If the acoustic wavelength is greater than the electronic mean free path, this transfer determines an effective viscosity, and the attenuation increases in proportion to the square of the frequency. When the mean free path becomes longer than the acoustic wavelength, as it does at low temperatures, the energy communicated to the electron is not returned to the

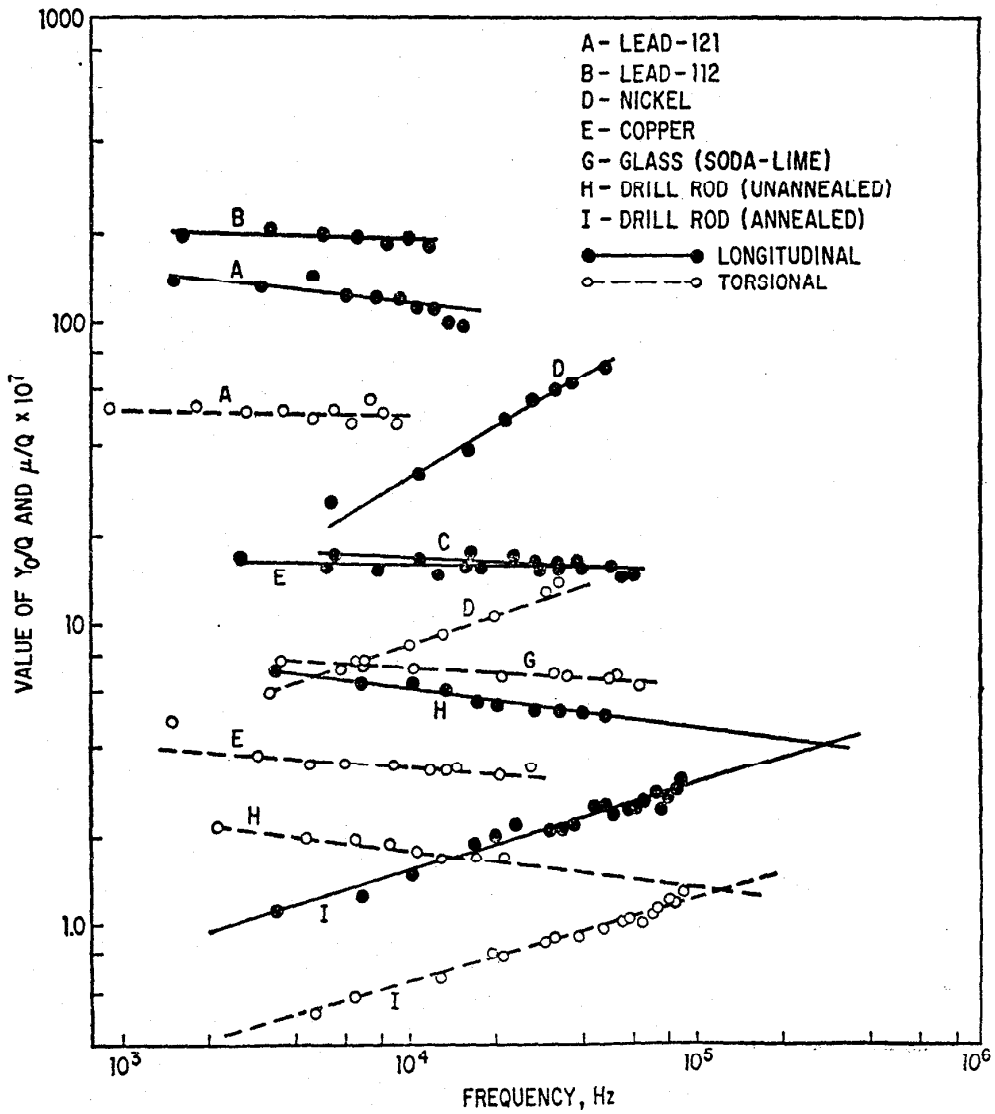

FIG. 3f-4. Values of Y_0/Q and μ/Q as function of frequency for a number of polycrystalline materials. (*After Wegel and Walther.*)

acoustic wave and a high attenuation results. The attenuation is proportional to the number of times the crystal lattice vibrates and hence to the frequency.

As the temperature drops below the temperature at which tin becomes superconductive (3.71 K), this source of attenuation drops rapidly to zero. The form of the curve has been used to confirm the Bardeen-Cooper-Schrieffer energy-gap theory of superconductivity. However, at lower frequencies—i.e., from 10 to 100 MHz—losses due to dislocations can occur. These are different for the normal and super-

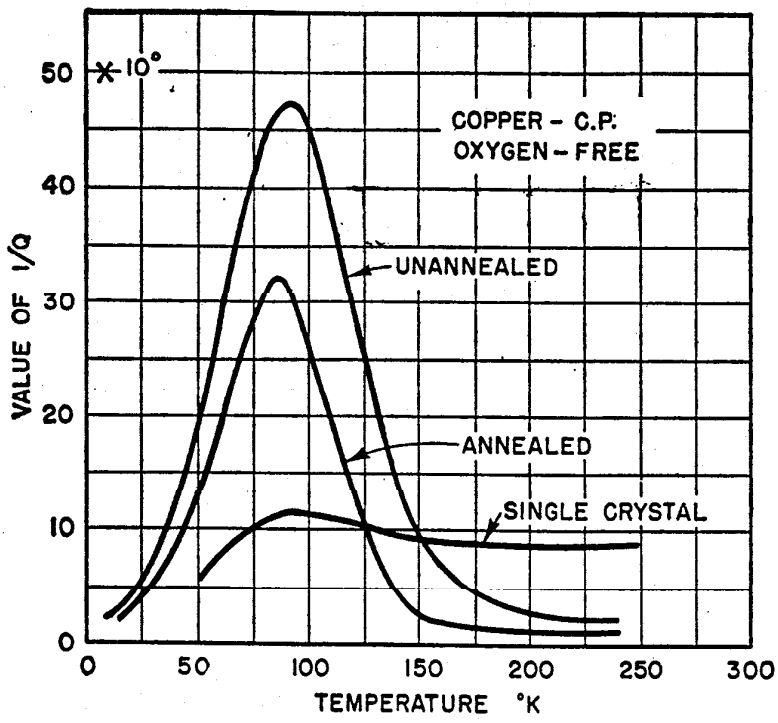

FIG. 3f-5. Attenuation peak in polycrystalline and single-crystal copper. (*After Bordoni.*

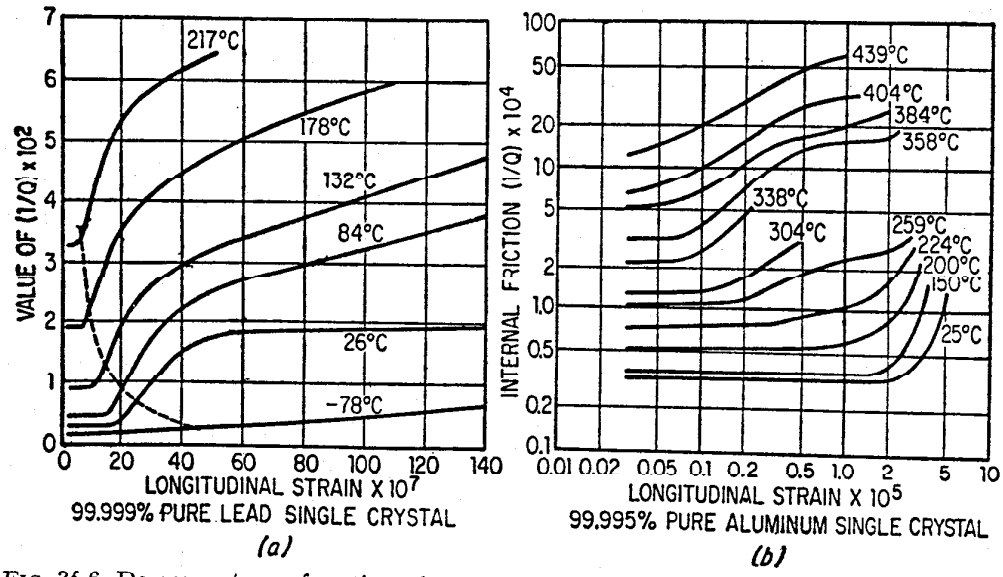

FIG. 3f-6. Decrement as a function of strain and temperature for single crystals of lead and aluminum.

conducting states, and this difference has to be taken account of in order to determine the form of the energy-gap relation. For frequencies above 100 MHz, the attenuation due to dislocations is small compared to the electron-phonon loss, and direct measurements give the shape of the energy-gap curves.

Acoustic measurements are also useful for type II or high-field superconductors (HFS).[1] For these types of superconductors—which are of use for superconducting

[1] See V. Shapira, "Physical Acoustics," vol. V, chap. 1, Academic Press, Inc., New York, 1968.

magnets—there are two critical fields—as shown by Fig. 3f-8—rather than the single field of type I superconductors. Figure 3f-8 compares the magnetization curves of type I and type II superconductors when the magnetic field H is directed along the axis of the cylinder. In type I the magnet flux is completely excluded from the interior of the material below H_c. For type II superconductors the magnetic flux

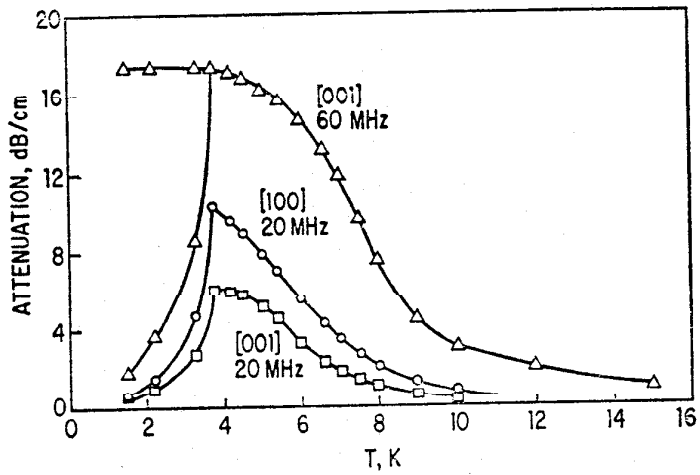

FIG. 3f-7. Longitudinal sound-wave attenuation measurements for a single crystal of tin along the [001] axis and along the [100] axis.

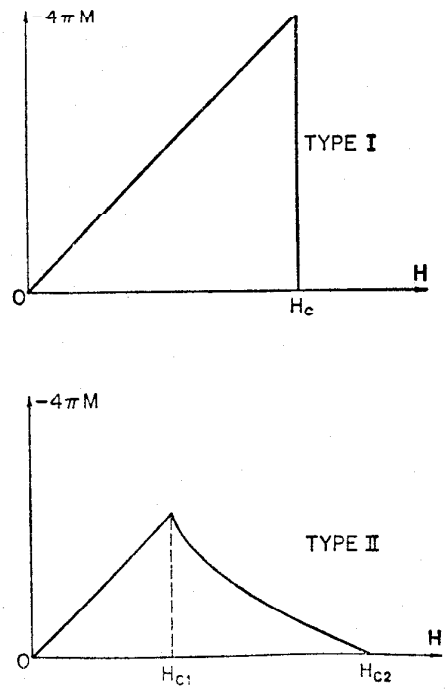

FIG. 3f-8. Magnetization curves of long cylinders of type I and type II superconductors. The applied field H is directed along the axis of the cylinder.

is completely excluded from the interior only below H_{c1}. Between H_{c1} and H_{c2} the magnetic flux consists of flux vortices in the form of filaments directed along H, embedded in a superconducting material. When a d-c electric current flows in a direction normal to H, each vortex experiences a force normal to its length which causes it to move. The vortices are pinned by defects, and it requires a finite current

density before the vortices move. An alternating current or alternating stress causes motions of the pinned vortices which lag behind the applied forces. The result is an acoustic attenuation. Figure 3f-9 shows the change in attenuation of a 9.1 MHz shear wave plotted as a function of the magnetic field. A sharp dip occurs near the

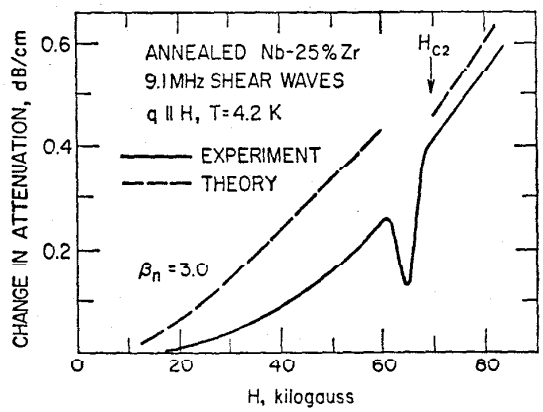

FIG. 3f-9. Magnetic-field variation of the attenuation of shear waves in annealed Nb–25 atom. % Zr at 4.2 K. Dashed curves are calculated values. (*After Y. Shapira.*)

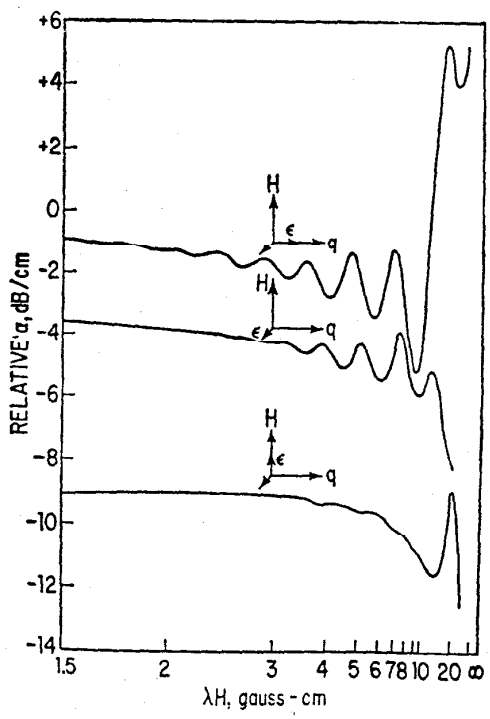

FIG. 3f-10. Relative attenuation in pure single-crystal copper as a function of the product of the wavelength times the magnetic field for several orientations of magnetic field and wave direction. (*After Morse.*)

superconducting field H_{c2}. Above H_{c2} the material is in the normal state, and the attenuation rises rapidly with the field.

Magnetoacoustics and Fermi Surface Determinations. In the presence of a magnetic field, the attenuation in metals in the normal state shows variations which are cyclic when plotted as a function of λH, where H is the magnetic field. Figure 3f-10 shows

measurements in a very pure copper single crystal at 4.2 K. These cyclic variations can be related to the shape of the Fermi surface, which is a constant-energy surface that bounds the occupied states of electrons in momentum space. The electrical effects in a metal are primarily determined by the electrons whose energy is near the Fermi surface, since these are the only ones free to move. For free electrons, such surfaces are spherical with a radius determined by the Fermi energy.

The effect of the periodic crystal potential in the band-theory approximation is to distort the Fermi surface from a spherical surface. Electrons of the same energy (which all lie on the Fermi surface) will then have different momenta. Figure 3f-11 shows the probable Fermi surfaces for monovalent copper, gold, and silver, and their relation to the Brillouin zone. If an electron's orbit in momentum space carries it

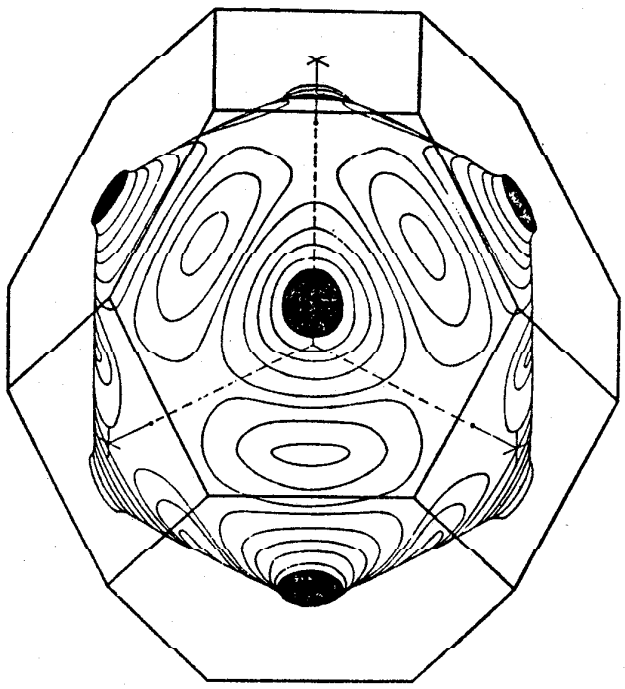

FIG. 3f-11. Fermi surfaces for copper, gold, and silver, and their relation to the Brillouin zone. (*After Pippard.*)

to the Brillouin zone face, the electron will be refracted to the opposite Brillouin zone face. In momentum space, this has the effect of repeating the zone over and over in an extended zone scheme. The effect of a magnetic field is to localize the electrons that can move onto a plane perpendicular to the magnetic field in momentum space. It can be shown that the periodicity of the attenuation-λH curves can be related to the linear dimension of the Fermi surface perpendicular to the magnetic field and perpendicular in momentum space to the direction of wave propagation in real space. The various measurements of Fig. 3f-10 give details of the Fermi surface for different directions in momentum space.

Several other types of oscillations in the attenuation occur.[1] These are the de Haas–van Alphen oscillations of the attenuation, the giant quantum oscillations, acoustic cyclotron resonance, and open orbit resonances.

[1] See B. W. Roberts, "Physical Acoustics," vol. IVB, chap. 10, Academic Press, Inc. New York, 1968.